



Intein-based Design Expands Diversity of Selenocysteine Reporters

Christina Z. Chung^{1‡}, Natalie Krahn^{1‡}, Ana Crnković^{1†} and Dieter Söll^{1,2*}

1 - Department of Molecular Biophysics and Biochemistry, Yale University, 266 Whitney Avenue, New Haven, CT 06511, USA

2 - Department of Chemistry, Yale University, 225 Prospect Street, New Haven, CT 06511, USA

Correspondence to Dieter Söll: *Department of Molecular Biophysics and Biochemistry, Yale University, 266 Whitney Avenue, New Haven, CT 06511, USA. christina.chung@yale.edu (C.Z. Chung), natalie.krahn@yale.edu (N. Krahn), ana.crnkovic@ki.si (A. Crnković), dieter.soll@yale.edu (D. Söll)

<https://doi.org/10.1016/j.jmb.2021.167199>

Edited by Tao Liu

Abstract

The presence of selenocysteine in a protein confers many unique properties that make the production of recombinant selenoproteins desirable. Targeted incorporation of Sec into a protein of choice is possible by exploiting elongation factor Tu-dependent reassignment of UAG codons, a strategy that has been continuously improved by a variety of means. Improving selenoprotein yield by directed evolution requires selection and screening markers that are titratable, have a high dynamic range, enable high-throughput screening, and can discriminate against nonspecific UAG decoding. Current screening techniques are limited to a handful of reporters where a cysteine (Cys) or Sec residue normally affords activity. Unfortunately, these existing Cys/Sec-dependent reporters lack the dynamic range of more ubiquitous reporters or suffer from other limitations. Here we present a versatile strategy to adapt established reporters for specific Sec incorporation. Inteins are intervening polypeptides that splice themselves from the precursor protein in an autocatalytic splicing reaction. Using an intein that relies exclusively on Sec for splicing, we show that this intein cassette can be placed in-frame within selection and screening markers, affording reporter activity only upon successful intein splicing. Furthermore, because functional splicing can only occur when a catalytic Sec is present, the amount of synthesized reporter directly measures UAG-directed Sec incorporation. Importantly, we show that results obtained with intein-containing reporters are comparable to the Sec incorporation levels determined by mass spectrometry of isolated recombinant selenoproteins. This result validates the use of these intein-containing reporters to screen for evolved components of a translation system yielding increased selenoprotein amounts.

© 2021 The Author(s). Published by Elsevier Ltd. This is an open access article under the CC BY-NC-ND license (<http://creativecommons.org/licenses/by-nc-nd/4.0/>).

Introduction

Selenium is an essential micronutrient in humans that exerts its health effects mainly through selenocysteine (Sec), the 21st amino acid.^{1,2} Chemically, Sec is equivalent to cysteine (Cys) with a selenium atom in place of the sulfur atom. However, the selenium atom provides Sec with unique properties.^{3,4} At physiological pH, Sec is consider-

ably more nucleophilic than Cys due to its lower pKa (5.2 vs 8.5), thus existing primarily in its ionized form while Cys is primarily found in its reduced form. In addition, Sec has been shown to be more resistant than Cys to inactivation by a variety of oxidizing reagents⁵ and forms a significantly stronger diselenide bond compared to its corresponding disulfide bond.⁶ Inserting Sec into recombinant proteins has chemical advantages,⁷ but it can also be used as a

tool for investigating reaction mechanisms, e.g., of redox enzymes,⁸ broadening its applications. Due to its high reactivity Sec is important in chemical protein synthesis,^{9,10} modulation of protein folding,^{11,12} and protein stability.⁶

Sec incorporation follows a pathway that is different from other amino acids, starting with synthesis on its cognate tRNA ($tRNA^{Sec}$) (Figure 1(A)). In bacteria, $tRNA^{Sec}$ (encoded by the *selC* gene) is serylated by seryl-tRNA synthetase (SerRS) and then serine (Ser) is converted to Sec by selenocysteine synthase (SelA). $Sec-tRNA^{Sec}$ is brought to the ribosome to decode an in-frame UGA codon by a specialized elongation factor, SelB, which interacts with a stem-loop structure (SECIS element) present in the Sec-encoding mRNA. This interaction and the specific distance between the UGA codon and the SECIS element create an appropriate context for natural UGA recoding and Sec insertion.¹³ Consequently, expression of archaeal and eukaryotic selenoproteins in which the SECIS element is located in the 3'-untranslated region may not be possible in *Escherichia coli*. However, changing the anticodon of *E. coli* $tRNA^{Sec}$ and keeping the SECIS present led to excellent yields for Sec-containing TrxR1 in the recoded C321.ΔA strain.¹⁴ Similarly, without additional mutations in their mRNA, the production of non-natural recombinant selenoproteins with Sec site-specifically inserted would not be feasible.

Alternate systems have been developed that utilize $tRNA^{Sec}$ variants to insert Sec in response

to UAG codons in *E. coli* (Figure 1(B)).^{15–18} These $tRNA^{Sec}$ variants are recognized by SerRS and SelA in a manner analogous to canonical $tRNA^{Sec}$ (Figure 1(A)) but are brought to the ribosome by EF-Tu. This removes the restriction placed by the SECIS element to dictate insertion of Sec at specific positions and allows the insertion of Sec anywhere in the protein. An important caveat with this technology is that EF-Tu is capable of binding Ser- $tRNA^{Sec}$, an intermediate in the pathway of $Sec-tRNA^{Sec}$ synthesis (Figure 1(B)).

As stop-codon read-through at a permissive site in GFP might occur via either Ser- $tRNA^{Sec}$ or $Sec-tRNA^{Sec}$ decoding, the amount of reporter activity correlates only with the extent of UAG read-through, and not insertion of Sec. For this reason, traditional genetic reporters employed to monitor incorporation of noncanonical amino acids at UAG codons are not suitable as reporters of Sec insertion. Accurate measurements of Sec insertion have thus far predominantly relied on the isolation and mass spectrometric analysis of the target protein for confirmation of Sec insertion.^{19,20}

Current Sec-specific reporters are limited to a small number of proteins where a Sec residue provides enzymatic activity. One common qualitative Sec-specific assay utilizes the ability of *E. coli* selenoenzyme formate dehydrogenase (FDH_H) to reduce benzyl viologen and generate a purple color.²¹ However, this assay is done under anaerobic conditions and requires an *E. coli* strain that carries deletions of the endogenous *fdhF* gene

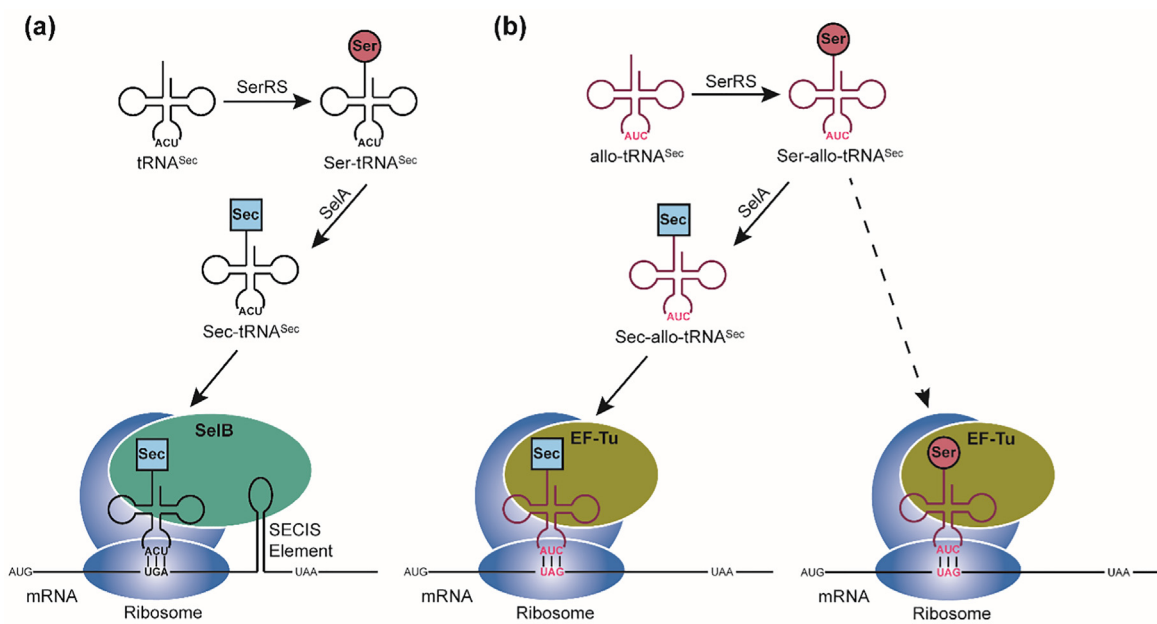


Figure 1. (a) Selenocysteine is formed on $tRNA^{Sec}$ using a combination of seryl-tRNA synthetase (SerRS) and selenocysteine synthase (SelA). The charged tRNA decodes a UGA codon through recognition of a Selenocysteine insertion sequences (SECIS) element by a specialized elongation factor (SelB). (b) In elongation factor Tu (EF-Tu) dependent translation, $allo-tRNA^{Sec}$ is recognized by SerRS and SelA, but is brought to the ribosome by EF-Tu to decode a UAG codon. Insertion of Ser is also possible (dashed line) due to recognition of Ser- $allo-tRNA^{Sec}$ by EF-Tu.

(encoding FDH_H) or components of the endogenous Sec insertion machinery.^{15–18} Analogous examination of Sec insertion through recombinant selenoprotein activity could be possible with, for example, human selenoprotein GPx1, but would be more laborious.^{15,16} To extend the repertoire of Sec-specific reporters, Cys-dependent proteins have been harnessed, provided that Cys replacement by Sec has significant effect on activity. Recently, a fluorescent Sec reporter²² was constructed from the phycobiliprotein (smURFP)²³ whose catalytic Cys is required for chromophore ligation. Appropriate intracellular heme levels are favorable for good fluorescence. The seleno-smURFP design replaces the catalytic Cys residue with Sec and provides a simple fluorescent method to distinguish between Sec and Ser.²²

Selection markers used for Sec-specific insertion include UAG-containing variants of thymidylate synthase (ThyA),¹⁵ human O⁶-alkylguanine-DNA alkyltransferase (hAGT),²⁴ and β-lactamase.^{18,22} These existing Sec-dependent reporters are gene specific, and rely on Sec incorporation for activity. They are limited in their dynamic range and suffer from toxicity, poor distinction from Ser, or the need to use anaerobic conditions.

Here, we present a versatile strategy to engineer established reporters to become Sec-dependent. This strategy is based on inserting an intein cassette in-frame within the reporter gene to disrupt protein activity, requiring intein splicing for functional capacity. Replacement of the catalytic Cys of this intein with Sec allows the production of an active reporter that directly measures UAG-directed Sec incorporation. The results below show that a DnaB mini-intein variant²⁵ was a suitable cassette to engineer such Sec-dependent reporters.

Results

Monitoring Sec incorporation via intein splicing – General strategy

To harness the power of general reporters such as superfolder green fluorescent protein (sfGFP) or antibiotic resistance genes for specific Sec insertion, we decided to use a Cys-dependent intein inserted in-frame within the reporter gene. Inteins may employ both Cys and Ser in their catalysis. The canonical splicing reaction requires Ser or Cys at the N-terminus of the intein (position 1, Figure S1) and Cys, Ser, or Thr at the N-terminus of the C-extein (position +1, Figure S1). The side chain in position 1 is necessary to start the splicing reaction by participating in the amide-thioester rearrangement that leads to the formation of the (thio)ester intermediate. The side chain in position +1 is necessary to execute the nucleophilic attack on the newly formed (thio)ester bond, facilitating the cyclization of the conserved Asn and subsequent

intein release (Figure S1).²⁶ Inteins have naturally evolved to work specifically within proteins they inhabit, resulting in drastically altered splicing activity when inserted into artificial protein targets.^{25,27,28}

Thus, we sought intein sequences whose catalytic activity is (i) independent of extein context and (ii) employ a catalytic Cys but not Ser at position 1. The *Synechocystis* sp PCC6803 DnaB intein was shortened to form a DnaB mini-intein consisting of only the essential amino acids required for protein splicing.²⁹ The protein was evolved to retain wild-type splicing activity when inserted into different sequences, with the most active and general variant identified as the M86 variant.²⁵ This protein efficiently splices only when Cys is present at position 1 of M86, but is inactive with Ser in this position (Figure 2). This feature is not common with all inteins, but one that is useful when investigating Sec incorporation (Ser misincorporation is possible when Sec conversion by Sela is inefficient (Figure 1(B)). Due to similar chemical reactivity of Cys and Sec, reassigning position 1 to Sec should also lead to protein splicing; thus, we generated a system that can distinguish between Ser and Sec at this crucial position (Figure 2). Following this approach, we can insert this DnaB mini-intein cassette into any gene and develop Sec-specific reporters that guide us to generate an enhanced selenoprotein translation system.

Creation of a Sec-specific selection marker

The Sec-specific selection systems used to date include thymidylate synthase, O⁶-alkylguanine-DNA alkyltransferase, and β-lactamase enzymes.^{15,18,22,24} Therefore we chose to work with a different reporter for selection, aminoglycoside-3'-phospho-transferase-I, the product of the kanamycin resistance (*kanR*) gene. This enzyme was already used to monitor intein splicing *in vivo* via a catalytic Cys residue at position 1.²⁵ To test the capability of this reporter to probe for Sec incorporation, we adapted the M86 DnaB mini-intein to encode Sec at position 1 and investigated insertion of the mini-intein at two different junctions (pAB_a01 and pAB_a02 plasmids; Figures 3(A and B)). Due to the possibility of Ser contamination in our Sec incorporation systems (Figure 1(B)), we required this reporter to be active with Sec and not Ser. For the initial experiment with Sec-mediated splicing, allo-tRNA^{UTu2D} was used;¹⁶ appropriate controls for Cys, Ser, and glycine (Gly) intein variants had this tRNA deleted. When M86 was inserted into the a01 site, Sec allowed growth up to 5 μg/mL kanamycin (kan), much less than the Cys containing reporter (20 μg/mL kan). However, when inserted into the a02 site of the KanR protein, Sec and Cys containing KanR-M86 proteins spliced equally well, allowing growth at wildtype (WT) levels (intein-free KanR protein, 20 μg/mL kan) (Figure 3(C)). Importantly, growth of pAB_a02 containing Ser or Gly (negative control)

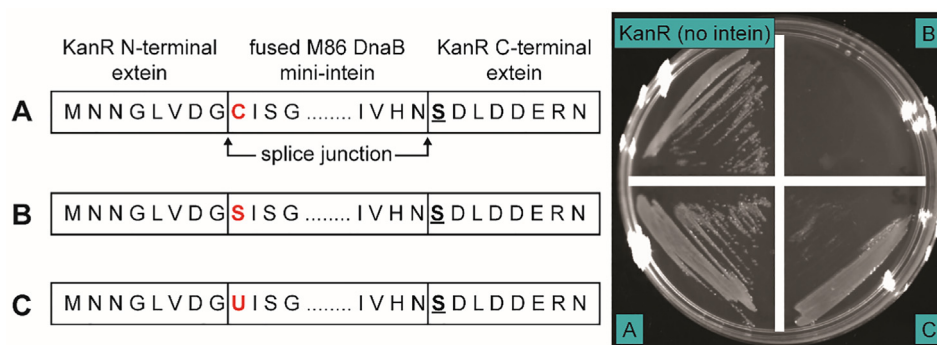


Figure 2. Schematic of the KanR-M86 reporter showing Cys (C), Ser (S), or Sec (U) at position 1 (bolded in red) and Ser (S) at position +1 (bolded and underlined). Successful splicing will result in complete removal of the intein and reconstitution of the functional KanR protein. The M86 DnaB mini-intein self-splices out of the KanR protein efficiently with Cys at position 1 (panel A), leading to growth comparable to the KanR protein lacking the intein (KanR (no intein)). Replacement of Cys with Ser (panel B) leads to inactive M86 that is unable to splice out to generate an active protein, while replacement with Sec (panel C) leads to efficient splicing. A representative image for 3 replicates is shown.

was equivalent (barely growing on 2.5 $\mu\text{g/mL}$ kan), while pAB_a01 containing Ser grew well to 10^{-1} dilution at the same kan concentration (more details on cell dilution are given in the legend to Figure 3). Considering the lower growth with Ser and higher activity with Sec, pAB_a02 was chosen for the remainder of the experiments.

After choosing a plasmid system specific for the presence of Sec (pAB_a02), we used it as a tool to determine which of our currently used cell lines is preferable for incorporation of Sec. Unfortunately, ME6 (*E. coli* $\Delta selABC \Delta fdhF$)¹⁶ was found to be a poor cell line in this assay, with the cells barely growing in the absence of kan (Figure S2(A)). In contrast, allo-tRNA^{UTu2D} facilitated growth up to 150 $\mu\text{g/mL}$ kan in B-95. $\Delta A \Delta fabR$ and B-95. $\Delta A \Delta fabR \Delta selABC$ strains,³⁰ comparable to the WT KanR protein and Cys containing pAB_a02 (Figures 3(D) and S2(B)). B-95. $\Delta A \Delta fabR \Delta selABC$ was further found to have less background growth (Gly present in position 1 allowed weak growth at 5 $\mu\text{g/mL}$ kan in B-95. $\Delta A \Delta fabR$) and therefore was chosen for the remainder of the experiments.

To show that incorporation of Sec is required for intein splicing, B-95. $\Delta A \Delta fabR \Delta selABC$ cells expressing the UAG variant of pAB_a02 and allo-tRNA^{UTu2D} were grown in either the presence or absence of 10 μM sodium selenite. Cells grown in the absence of sodium selenite could not grow on plates containing 20 $\mu\text{g/mL}$ kan while the addition of sodium selenite allowed growth (Figure S3(A)). Growth of cells up to 5 $\mu\text{g/mL}$ kan in the absence of sodium selenite is likely due to the presence of a selenium source in the growth media.

Furthermore, we demonstrate that the KanR-M86 system can detect minor differences in tRNA expression. B-95. $\Delta A \Delta fabR \Delta selABC$ cells grown under different arabinose concentrations (to induce allo-tRNA^{UTu2D}) showed that increasing tRNA levels allowed growth on plates with higher

concentrations of kanamycin (Figure S3(B)). Cells grown in the presence of 0.001% arabinose could not grow at 50 $\mu\text{g/mL}$ kan while 0.1% arabinose allowed growth up to 150 $\mu\text{g/mL}$ kan.

Adaptation of a GFP reporter for specific Sec incorporation

To show the versatility of the intein-based design for engineering another Sec-specific reporter, we applied it to the commonly used fluorescent screening reporter, sfGFP. As discussed above, seleno-smURFP²² is highly selective for Sec; yet very low fluorescence is still possible with the Ser variant. However, with the intein-based design, we can completely exclude Ser incorporation, as this amino acid prevents protein splicing.

To design the sfGFP-M86 reporter, we tested M86 splicing with four sfGFP-M86 fusion proteins (Figures 4(A and B)). Intein insertion positions were strategically chosen to interrupt a β -sheet and disrupt the fluorescent properties of the protein, requiring intein splicing for fluorescence. In all cases the M86 sequence was introduced preceding a naturally occurring Ser, except for pB_03, where a natural Arg was mutated to Ser (Ser is found in the WT GFP sequence). In this way the Ser residues of sfGFP occupy position +1 which is crucial for splicing (Figure S1). To mimic standard recombinant protein expression, we adopted an inducible plasmid system (pB_sfGFP) (Figures 4(A and B)). We tested the efficiency of M86 splicing at the four positions using a catalytic Cys at position 1 (Figure 4(C)). Compared to WT sfGFP (without intein), the best performing construct (pB_04) showed approximately 30% fluorescent intensity. The remaining constructs (pB_01, pB_02, pB_03) showed lower, mutually comparable yields of about 10% fluorescent intensity of WT sfGFP. As with the KanR-M86

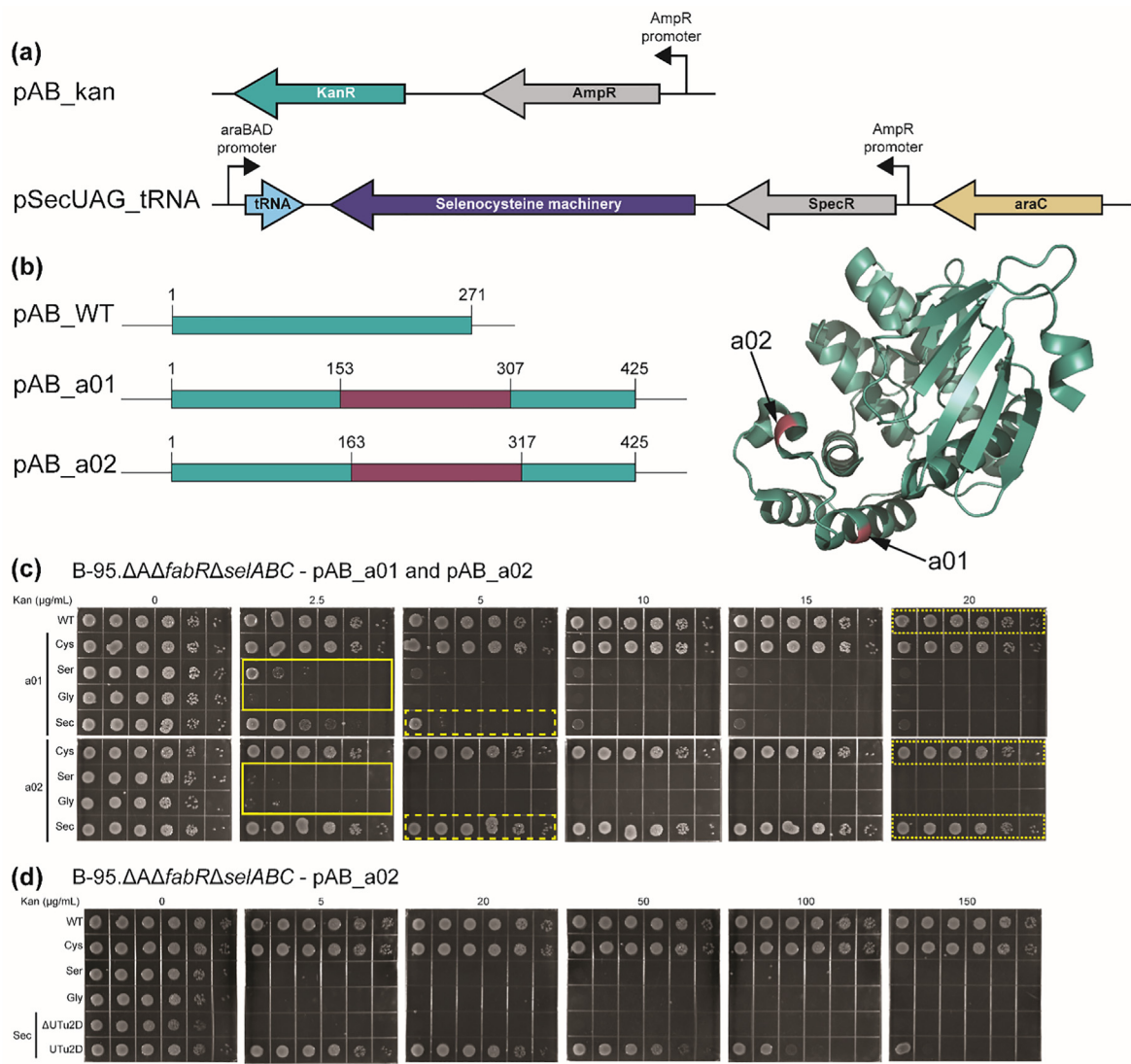


Figure 3. (a) Design of the plasmids used to test the Sec incorporation by different tRNA variants using the kanamycin resistance (*kanR*) gene. (b) The M86 intein (highlighted in purple) was inserted at two different positions (a01 and a02)²⁵ in the *kanR* gene that would disrupt protein function (PDB ID: 4EJ7).³⁵ (c) The M86 intein was tested for efficiency in splicing at positions a01 and a02 with Cys or Sec at position 1 and growth was compared to the wildtype (WT) KanR protein without the intein. Position 1 was also mutated to Ser or Gly to confirm absence of splicing. Initial spots are at $A_{600} = 2.0$ with 10-fold dilutions across the plate. Each plate is at a different concentration of kanamycin (0–20 μg/mL). (d) pAB_a02 was chosen to test the efficiency of Sec incorporation in B-95. ΔAΔfabRΔselABC. A pSecUAG_tRNA plasmid lacking allo-tRNA^{UTu2D} (ΔUTu2D) was used as a negative control. Each plate is at a different concentration of kanamycin (0–150 μg/mL). Areas of importance to compare are boxed in the same yellow line pattern. Representative images for 3 replicates are shown.

assay, we tested pB_04 in three different *E. coli* strains: ME6, B-95.ΔAΔfabR, and B-95. ΔAΔfabRΔselABC. Since the fluorescence was comparable for the latter two strains, B-95. ΔAΔfabRΔselABC was chosen as it lacks the endogenous Sec machinery and is the same strain that was used for the KanR-M86 assays.

Next, we tested the performance of pB_04 as a Sec-specific reporter (Figure 4(D)). We introduced a UAG codon in place of the catalytic Cys (position 1) of M86 and co-transformed this

construct with the pSecUAG_tRNA plasmid (containing the necessary Sec incorporation machinery and allo-tRNA^{UTu2D}). Under the conditions necessary for optimal Sec incorporation, Sec-dependent splicing (U) and sfGFP fluorescence was ~30% of the Cys-containing construct (C) (Figure 4(D)). Importantly, pB_04 variants containing Ser (S) or Gly (G) showed no fluorescence when tested. This confirms the usefulness of sfGFP-M86 as a suitable reporter for Sec-specific insertion.

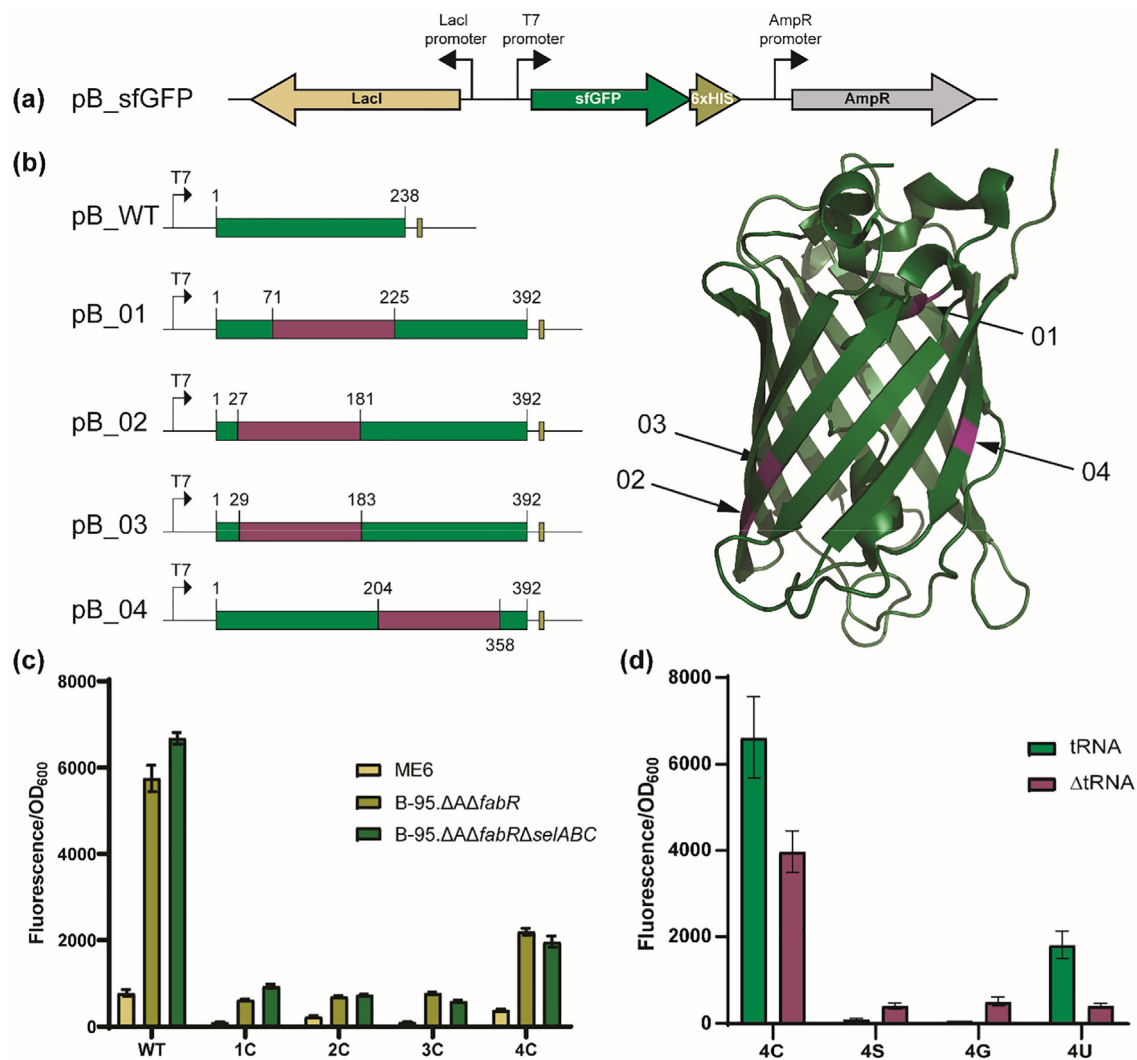


Figure 4. (a) Design of plasmid used to encode sfGFP. This plasmid, in combination with the pSecUAG_tRNA plasmid, was used to test Sec incorporation by different tRNA variants. (b) The M86 intein (highlighted in purple) was inserted at four different positions in the sfGFP gene that would disrupt protein function (PDB ID: [2B3P](#)).³⁶ (c) Splicing efficiency of M86 intein was tested at all four positions in three cell lines (ME6, B-95.ΔAΔfabR, and B-95.ΔAΔfabRΔsel/ABC) with Cys (C) at position 1 compared to the wildtype (WT) sfGFP protein without the intein. (d) Sensitivity of pB_04 to Ser (S) and Gly (G) was tested and compared to Cys (C) and Sec (U) with allo-tRNA^{UTu2D}. A pSecUAG_tRNA plasmid lacking allo-tRNA^{UTu2D} (ΔtRNA) was used as a negative control. Values shown are the average and standard deviation of four biological replicates.

Application of the Sec reporters using known tRNA^{Sec} variants to compare Sec incorporation

Current EF-Tu dependent Sec insertion systems are still lacking with respect to protein yield. In one case *E. coli* Hyd-1 with a single Sec residue produced yields of only 6% that of the Cys-containing Hyd-1.⁸ Therefore, further optimizations of EF-Tu dependent Sec insertion systems are necessary. To emphasize the ability of these intein-based reporters to screen for a better Sec incorporation system, we employed already optimized tRNA^{Sec} variants and their respective machineries. For 13-branch systems, tRNA^{SecUX}

and tRNA^{UTux} contained the compatible *E. coli* SelA enzyme,^{17,18} while the 12-branch allo-tRNA-derived variants (allo-tRNA^{UTu1}, allo-tRNA^{UTu1D}, allo-tRNA^{UTu2}, and allo-tRNA^{UTu2D}) contained the *Aeromonas salmonicida* SelA and SelD enzymes (Figure S4).¹⁶ Figure 5(A) shows that the KanR-M86 reporter is able to distinguish small changes in Sec incorporation efficiency over a wide range of kan concentrations. We observed allo-tRNA^{UTu1}, allo-tRNA^{UTu1D}, and allo-tRNA^{UTu2D} to grow well at high concentrations of kan (100–150 μg/mL) (Figure 5(A)). Allo-tRNA^{UTu1D} was found to grow at multiple dilutions (up to 10⁻⁴) at 150 μg/mL kan while allo-tRNA^{UTu1} and allo-tRNA^{UTu2D} only survived

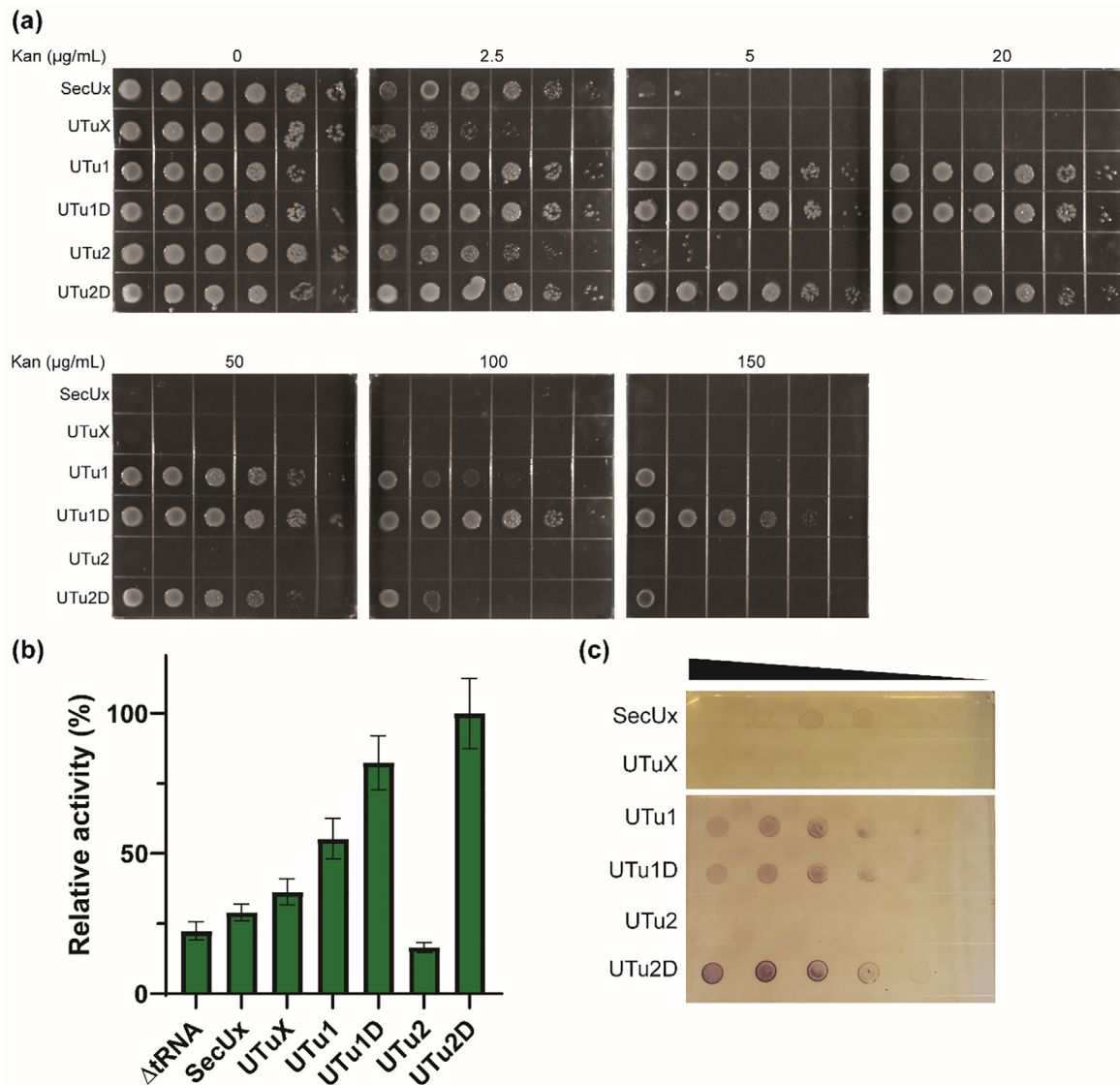


Figure 5. (a) KanR-M86 assay using pAB_a02 to test efficiency of six tRNA^{Sec} variants. Initial spots are at A₆₀₀ = 2.0 with 10-fold dilutions across the plate. Each plate contains a different concentration of kanamycin (0–150 µg/mL). (b) sfGFP-M86 assay using pB_04 to test efficiency of the same six tRNA^{Sec} variants. Values shown are the average and standard deviation of 8 biological replicates. (c) Benzyl viologen assay using *E. coli* FDH_H (140UAG) to test the efficiency of six tRNA^{Sec} variants. Initial spots are at A₆₀₀ = 5.0 with 2-fold dilutions across the plate. Plates shown are representatives of greater than 3 replicates.

when undiluted (more details on cell dilution are given in the legend to Figure 5). On the other hand, tRNA^{SecUx}, tRNA^{UTuX}, and allo-tRNA^{UTu2} barely supported growth at 2.5–5 µg/mL kan.

Comparable results are obtained with the sfGFP-M86 reporter. Maximum fluorescence was obtained using allo-tRNA^{UTu1D} and allo-tRNA^{UTu2D}, with allo-tRNA^{UTu1} hovering around 50% that of allo-tRNA^{UTu2D} (Figure 5(B)). On the other hand, relative activity of tRNA^{SecUx}, tRNA^{UTuX}, and allo-tRNA^{UTu2} was between 25–30%, around the level of background fluorescence (Δ tRNA plasmid).

These results are in an agreement with Sec incorporation levels as monitored by the benzyl

viologen assay (Figure 5(C)). The *E. coli* fdhF gene, encoding FDH_H, produces active protein only when position 140 contains a Sec residue. Active protein is verified by reduction of benzyl viologen under anaerobic conditions to produce an observable purple color. Using an inducible expression system (similar to the pB_sfGFP reporter), we tested all the tRNAs investigated with the intein-based reporters. Allo-tRNA^{UTu2D} allowed the strongest purple color to be developed at dilutions up to 2⁻³ while strains harboring allo-tRNA^{UTu1} and allo-tRNA^{UTu1D} both had a weaker color, although equivalent to one another. Parallel to what was observed in the previous assays,

under these conditions no accumulation of purple color was observed for tRNA^{SecUx}, tRNA^{UTuX}, and allo-tRNA^{UTu2}.

Sec incorporation measured by mass spectrometry matches results from intein-based reporters

To verify that the results obtained through *in vivo* assays using the intein-based reporters correlated with selenoprotein expression levels, we expressed and purified two selenoproteins, *E. coli* Grx1 and human GPx1, using the EF-Tu dependent Sec incorporation technology (Table 1 and Figure 1(B)). Recombinant selenoprotein expression levels were tested employing various tRNA^{Sec} variants and their respective machineries. Using the same expression and purification protocol for both proteins, we were able to compare the trends of the protein yields observed between the tRNAs.

The trend of protein yields was consistent between Grx1 and GPx1, with the exception of allo-tRNA^{UTu1} (Table 1). Allo-tRNA^{UTu1D} facilitated the highest yield while tRNA^{UTuX} resulted in the lowest (in descending order allo-tRNA^{UTu1D} > tRNA^{SecUx} > allo-tRNA^{UTu2D} > allo-tRNA^{UTu2} > tRNA^{UTuX}). Allo-tRNA^{UTu1} was found to have the highest yield in Grx1 (twice that of allo-tRNA^{UTu1D}) but the lowest in GPx1 (equivalent to tRNA^{UTuX}).

The more important question was whether the recombinant selenoproteins were active and how much Sec was incorporated. Both Grx1 and GPx1 produced similar trends for enzymatic activity with allo-tRNA^{UTu1D} having the highest activity and tRNA^{UTuX} having the lowest (in descending order allo-tRNA^{UTu1D} > allo-tRNA^{UTu1} > allo-tRNA^{UTu2D} > allo-tRNA^{UTu2} > tRNA^{SecUx} > tRNA^{UTuX}) (Table 1). To confirm that the enzymatic activity correlated to the amount of Sec inserted, intact mass spectrometry (MS) of the proteins was done. Deconvolution of the MS spectra found that the percentage of Sec in the

proteins correlated with its observed activity; higher percentage of Sec leads to increased activity (Table 1, Figures 6 and 7). For Grx1, allo-tRNA^{UTu1} Sec incorporation was low compared to its activity. This discrepancy can be explained by the difficulty in distinguishing the overlapping peaks due to Grx1_Q11 with one oxidation and Grx1_U11. It should be noted that Grx1 is naturally not a selenoprotein and its Cys homolog (positive control) is more active than when Sec is present. GPx1 is a natural selenoprotein and replacement of the active site Sec for Cys deems it inactive.³¹ The amount of Sec incorporation varied between the proteins, though the trend remained the same. tRNAs which had low Sec incorporation in the intein-based assays were found to have a higher percentage of Sec incorporated in Grx1 compared to GPx1. However, for tRNAs with high Sec incorporation in the intein-based assays (allo-tRNA^{UTu1} and allo-tRNA^{UTu1D}), GPx1 had a higher amount of Sec (44.9% and 73.4%, respectively) compared to Grx1 (19.1% and 33.7%, respectively).

The MS and enzymatic activity of these recombinant selenoproteins agrees with most of the results obtained from the intein-based reporters. From the sfGFP-M86 and benzyl viologen assay, allo-tRNA^{UTu2D} stands out as a promising candidate for Sec incorporation. However, it did not produce reasonable Sec incorporation in either Grx1 or GPx1. Instead, allo-tRNA^{UTu1D} performed well in both intein-based reporters and the benzyl viologen assay, affording the highest Sec incorporation in both recombinant selenoproteins.

Discussion

The many desirable applications of selenoproteins drive the desire to improve the current methodologies for site-specific *in vivo* Sec incorporation. Two top aims, increased selenoprotein yields and consistently high levels of Sec incorporation require Sec-specific selection tools and screening reporters with high dynamic

Table 1 Table of values for Grx1 and GPx1 production with various tRNAs for Sec incorporation.

tRNA	Grx1			GPx1		
	Yield (mg)*	Sec incorporation (%)	Activity (U/mg)**	Yield (mg)*	Sec incorporation (%)	Activity (U/mg)**
SecUx	0.42	13.6	9 ± 2	0.40	6.8	0.08 ± 0.01
UTuX	0.15	18.8	4 ± 2	0.18	0	0.28 ± 0.03
UTu1	3.8	19.1	35 ± 4	0.18	44.9	21 ± 4
UTu1D	1.6	33.7	53 ± 4	0.62	73.4	29 ± 2
UTu2	0.30	19.0	9 ± 2	0.21	ND	1.2 ± 0.3
UTu2D	0.37	31.8	25 ± 3	0.26	11.5	5 ± 1
Pos Control	ND	0	130 ± 10	ND	100	32 ± 3
Neg Control	ND	0	2 ± 1	ND	0	0.07 ± 0.01

ND: not determined.

* Protein yield is from a 1 L culture.

** 1 U is defined as the amount of enzyme that catalyzes conversion of 1 μmol of substrate per minute at 25 °C ± SE.

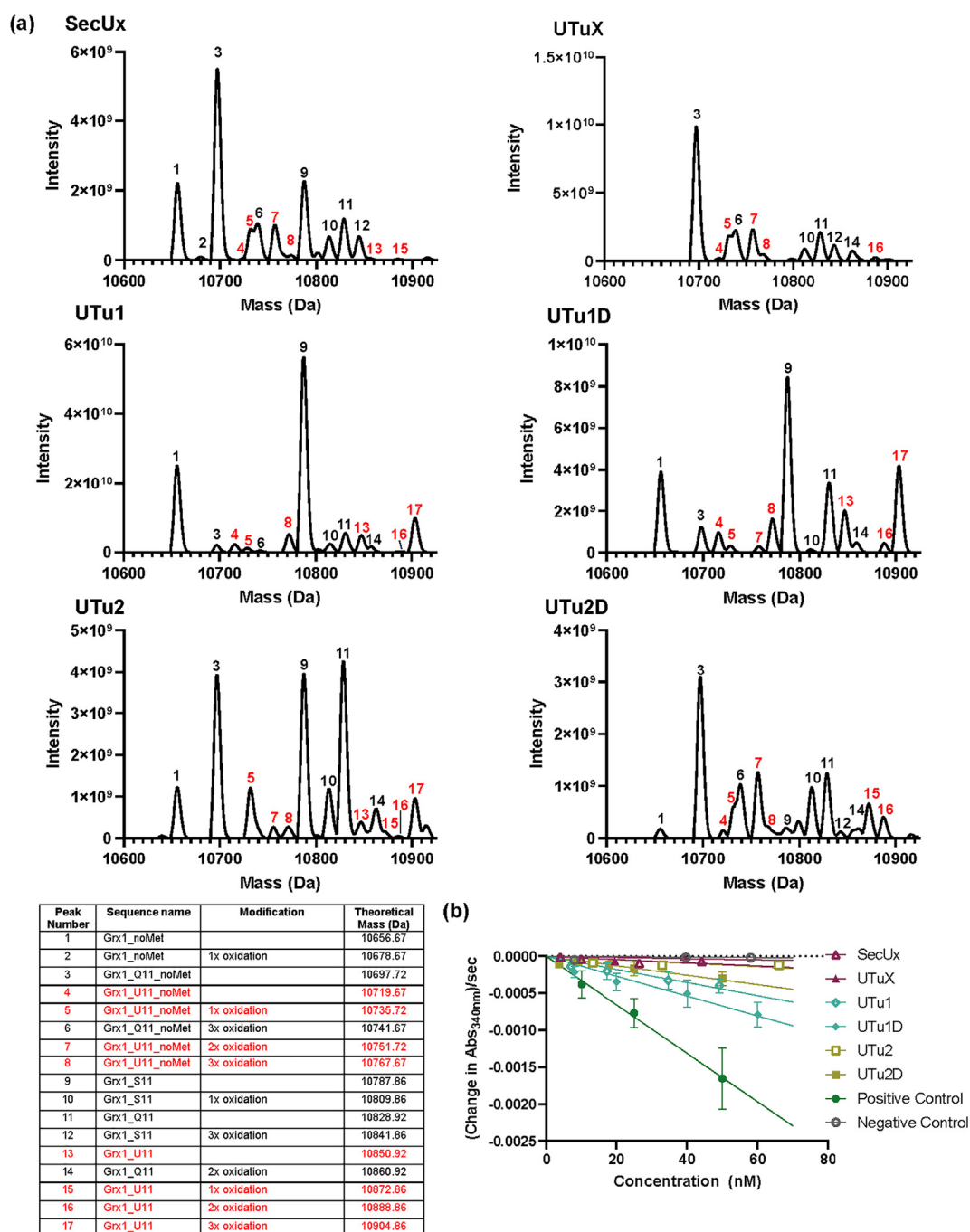


Figure 6. (a) Intact mass analysis of Grx1 to determine the amount of selenocysteine (Sec, U) incorporation for each tRNA tested with the intein-based reporters. Peaks corresponding to Sec incorporation are highlighted in red while serine (S) and glutamine (Q) incorporation are in black. The table below the spectra provides details on the identified peaks. (b) Grx1 activity assay for each tRNA^{Sec} variant was visualized as the consumption of NADPH over time at concentrations up to 65 nM of a tRNA^{Sec} variant. Data points are an average of three independent measurements \pm SD.

range. The currently accepted method to confirm Sec incorporation is through expressing FDH_H and testing its activity via benzyl viologen reduction.²¹ This very sensitive method detects even the smallest amount of Sec incorporation, but requires work in an anaerobic chamber. A β -lactamase reporter

used to screen a library of tRNA^{Sec} variants required up to 1000 μ g/mL ampicillin,¹⁸ much higher than the recommended working concentration, to screen for a tRNA species with low Sec incorporation (tRNA^{SecUx}) (Table 1). Recently seleno-smURFP has provided a quantitative fluorescent

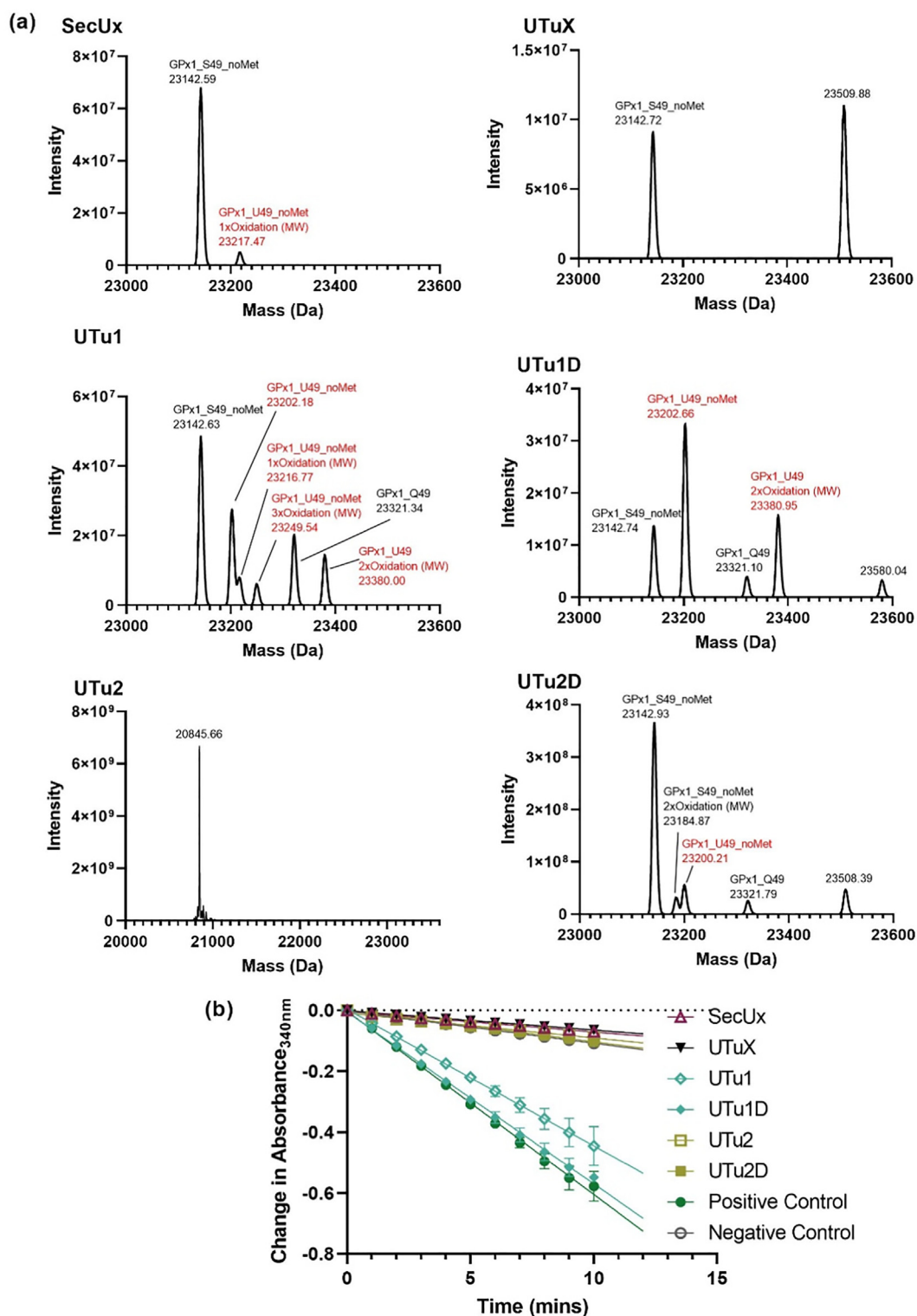


Figure 7. (a) Intact mass analysis of GPx1 to determine the amount of selenocysteine (Sec, U) incorporation for each tRNA tested with the intein-based reporters. Peaks corresponding to Sec incorporation are highlighted in red while serine (S) and glutamine (Q) incorporation are in black. No peaks were observed at the correct size for allo-tRNA^{UTu2}. The truncated product detected in the intact mass analysis of GPx1 expressed in the presence of allo-tRNA^{UTu2} was observed in all spectra (not shown). (b) GPx1 activity assay for each tRNA^{Sec} variant was visualized as the consumption of NADPH over time. Data points are an average of three independent measurements \pm SD.

reporter that has been used to improve genetically recoded *E. coli* strains for selenoprotein production.²² However, this reporter requires special optimization of the bacterial strain, and is poor at discriminating against Ser incorporation.

The potential use of inteins as Sec-specific reporters was already demonstrated by our group and others: *Mycobacterium xenopi* GyrA intein is active when the catalytic Cys is replaced by Sec, but not Ser.^{16,24,32} However, the GyrA intein activity was induced *in vitro*, in the presence of high concentrations of dithiothreitol. For the purposes of an *in vivo* Sec-reporter assay, we sought an intein that would be (i) catalytically active once Sec is introduced, (ii) inactive when the catalytic residue is replaced by Ser, and (iii) tolerant towards the surrounding extein sequences. The first two conditions had to be satisfied to monitor specific Sec insertion, as well as Ser misincorporation. The third condition was critical to generate a Sec-specific cassette that could be shuttled between different reporters.

The DnaB mini-intein M86 showed remarkable sensitivity to Ser insertion and is catalytically active in the presence of Sec (Figure 2). Furthermore, it had been previously evolved to perform as a general intein, with the ability to splice different proteins at multiple insertion sites.²⁵ Since splicing activity is not equal at each insertion site, this allows the reporter to be easily tuned to extend its dynamic range. Starting with a Sec system that is not very efficient, we optimized the insertion site to achieve the highest signal while maintaining sensitivity for Sec incorporation (a02 for the KanR protein and 04 for sfGFP; Figures 3(C–D), 4(C–D), and S2).

With these two different reporter systems, we were able to test the activity of various tRNAs previously used for Sec incorporation. Comparing the various Sec-tRNAs, $\text{allo-tRNA}^{\text{UTu1}}$, $\text{allo-tRNA}^{\text{UTu1D}}$, and $\text{allo-tRNA}^{\text{UTu2D}}$ produced greater selenoprotein amounts than $\text{tRNA}^{\text{SecUx}}$, $\text{tRNA}^{\text{UTuX}}$, and $\text{allo-tRNA}^{\text{UTu2}}$ (Table 1 and Figures 6 and 7). The top three performing tRNAs, $\text{allo-tRNA}^{\text{UTu1D}}$, $\text{allo-tRNA}^{\text{UTu1}}$, and $\text{allo-tRNA}^{\text{UTu2D}}$ enabled cells to develop significant kan resistance and fluorescence. The slightly different results between the performance of these tRNAs in the two assays can be attributed to context-dependent tRNA suitability, *i.e.* the mRNA-tRNA interaction, and differences in the way each reporter is expressed; KanR-M86 uses a constitutive promoter, while sfGFP-M86 expression is induced. The latter system allows a more stringent control over expression of the reporter. With addition of arabinose at the beginning of the culture, cells are first allowed to produce large quantities of tRNA^{Sec} , which are subsequently serylated by endogenous SerRS, before converted to Sec by the plasmid borne copy of SelA. In this way, the pool of acylated suppressor tRNA is created prior to expression of the reporter.

In the case of KanR-M86, the constitutively expressed mRNA can be translated at an earlier time point, potentially using more of the $\text{Ser-tRNA}^{\text{Sec}}$ intermediate. This may mask the subtle differences in the efficiency of Ser-to-Sec conversion between different tRNAs. Specifically, both $\text{allo-tRNA}^{\text{UTu1D}}$ and $\text{allo-tRNA}^{\text{UTu2D}}$ have been altered in their D-arm to have a higher affinity to *A. salmonicida* SelA than their previous variants ($\text{allo-tRNA}^{\text{UTu1}}$ and $\text{allo-tRNA}^{\text{UTu2}}$, respectively) (Figures 5(B) and S4).¹⁶ It is likely that this improved conversion of the reaction intermediate is more apparent in the sfGFP-M86 assay due to the controlled expression of the reporter.

Protein expression of Grx1 and GPx1 confirmed that $\text{allo-tRNA}^{\text{UTu1D}}$ produced the highest yield with the most Sec incorporated. The yield of Sec incorporated using $\text{allo-tRNA}^{\text{UTu1}}$ was protein dependent; significantly higher than $\text{allo-tRNA}^{\text{UTu2D}}$ in GPx1 compared to Grx1 (Table 1, Figures 6 and 7). This was also observed in the two intein assays, with $\text{allo-tRNA}^{\text{UTu1}}$ performing better in the KanR-M86 compared to the sfGFP-M86 assay (Figures 5(A and B)). However, this was not the case with $\text{allo-tRNA}^{\text{UTu2D}}$. $\text{Allo-tRNA}^{\text{UTu2D}}$ exhibited low to modest Sec incorporation in GPx1 and Grx1 compared to $\text{allo-tRNA}^{\text{UTu1}}$ and $\text{allo-tRNA}^{\text{UTu1D}}$ (Table 1, Figures 6 and 7) while displaying the highest Sec incorporation in the sfGFP-M86 assay (Figure 5 (B)) and benzyl viologen assay (Figure 5(C)). This is likely due the dependence of $\text{allo-tRNA}^{\text{UTu2D}}$ on the sequences surrounding the recoded UAG codon. Thus, application of both intein-based reporters is preferred to identify the best performing tRNA variants (or Sec incorporation system) before expression of the desired selenoprotein.

This strategy of designing intein reporters is not limited to the KanR protein or sfGFP, but applicable to any gene of interest. In addition, the assay sensitivity can be altered by choosing a different intein insertion position in the protein. We tested out positions a01 and a02 for the KanR-M86 reporter as they had the highest splicing activity (Figure 3(C)). However, as the Sec incorporation system becomes more efficient, a reasonable concentration of kan may not be sufficient for selection. Therefore, by inserting the intein at a different position,²⁵ the kan concentration may be reduced for appropriate selection. The ability to choose the gene and tune the sensitivity of the reporter makes it a versatile tool for synthetic biologists to engineer efficient machinery for Sec incorporation.

Although our studies were performed in *E. coli*, the intein reporter system is not limited to bacteria. Using the same strategy as described above, an appropriate reporter may be designed for use in eukaryotes, specifically in mammalian cells. There are currently 25 identified selenoproteins in

humans, with many of their functions still unknown.¹ Human proteins can be difficult to produce in *E. coli* and will lack the proper posttranslational modifications, among other problems,³³ hindering our study of selenoproteins. Designing a recombinant Sec system in mammalian cells would allow overexpression of the proteins with the proper modifications for protein activity and folding. As the mammalian Sec incorporation system is quite complicated (*i.e.* more components compared to the bacterial system and unidentified factors in the pathway), a simple fluorescent intein-based reporter that relies solely on the incorporation of Sec without affecting endogenous machinery, should help in the development of a recombinant Sec system.

Materials and methods

Cloning and mutagenesis

KanR-M86 expression plasmids. Plasmids encoding aminoglycoside-3'-phosphotransferase-I, the kanamycin resistance (*kanR*) gene with the M86 DnaB mini-intein variant inserted after Ser154 and Ser164 (pAB_a01 and pAB_a02, respectively; Table S1) were kindly provided by Henning D. Mootz.²⁵ Position 1 of the intein (Cys, TGC) was mutated to encode Ser (TCG), Gly (GGT in pAB_a01, GGC in pAB_a02), or Sec (TAG) in both plasmids. All PCRs were performed with *PfuUltra II Fusion HS DNA Polymerase* (Agilent). PCR products were gel purified (Macherey-Nagel) and ligated together using NEBuilder[®] HiFi DNA Assembly Master Mix (NEB). Products were transformed into DH5 α competent cells and sequencing of the plasmids confirmed successful mutagenesis (Quintara Biosciences).

A control plasmid with wild-type *kanR* lacking the intein (pAB_kan) was generated by amplifying pAB_a02 around the intein. The PCR products were gel purified (Macherey-Nagel) and the linear products were 5'-end phosphorylated and ligated in the same reaction using T4 PNK (NEB) and T4 DNA ligase (NEB), respectively. Products were transformed into DH5 α competent cells and sequencing of the plasmids confirmed successful removal of M86 (Quintara Biosciences).

Sec system expression plasmids. Construction of all plasmids encoding the Sec expression system used in this study have been previously reported.¹⁶ The pSecUAG-ADT series was used with allo-tRNA^{UTu1}, allo-tRNA^{UTu1D}, or allo-tRNA^{UTu2} and the pSecUAG-Evol series was used for allo-tRNA^{UTu2D}. For tRNA^{SecUx} and tRNA^{UTuX}, plasmids with the same backbone as the pSecUAG-Evol and ADT series were used but with the *E. coli* Sec machinery (pSecAUG_tRNA plasmids). The *kanR* gene was replaced with *specR* to allow co-transformation with the KanR-M86 constructs. A control plasmid was generated by delet-

ing allo-tRNA^{UTu2D} in the same manner as described above.

sfGFP-M86 expression plasmids. *E. coli* codon-optimized sfGFP with a C-terminal His₆-tag was amplified and inserted into pET-15b in place of the N-terminal His₆-tag, thrombin site, and multiple cloning site. The inserted sfGFP gene along with the T7 promoter, T7 terminator, and *lacI* sequences was amplified and moved to the high-copy number plasmid pBAD, where it replaced the araBAD promoter. The M86 DnaB mini-intein was inserted after residues 27, 29, 71, and 204 (Table S1 and Figure 4(B)) and site-directed mutagenesis was performed to mutate position 1 (Cys, TGC) of the intein to encode Ser (AGC), Gly (GGC), or Sec (TAG) (pB_sfGFP series).

E. coli Grx1 and human GPx1 expression plasmids. Construction of pET-Grx1(11UAG/14Ser), pET-Grx1(11Cys/14Ser), pET-GPx1(49UAG), and pET-GPx1(49Cys) has been previously described.¹⁶ pET-Grx1(11Ser/14Ser) was constructed through site-directed mutagenesis following manufacturer's instructions to change TAG to AGC.

E. coli FDH_H expression plasmids. *E. coli fdhF* gene was cloned into pTRC99A with a C-terminal His₆-tag. Position 140 (TGA) encodes Sec and was mutated to TAG through site-directed mutagenesis.¹⁶

Kanamycin resistance assay

Plasmids encoding the Sec expression system and KanR-M86 variant were transformed into electrocompetent *E. coli* cells (ME6, B-95. $\Delta A\Delta fabR$, or B-95. $\Delta A\Delta fabR\Delta selABC$),^{16,30} plated on LB agar plates (50 μ g/mL ampicillin, 50 μ g/mL spectinomycin), and incubated at 37 °C overnight. Single colonies were grown in 5 mL LB cultures (50 μ g/mL amp, 50 μ g/mL spec, 0.1% arabinose, 10 μ M sodium selenite (Na₂SeO₃)) at 37 °C overnight. A dilution to A₆₀₀ 2.0 and 10-fold serial dilutions were prepared. From each dilution, 5 μ L was spotted onto LB agar plates (50 μ g/mL amp, 50 μ g/mL spec, 0.1% arabinose, 10 μ M Na₂SeO₃) containing 0–150 μ g/mL kan. Plates were left at 37 °C overnight and imaged the next day on the ChemiDoc[™] MP Imager (Bio-Rad). For streaked cells, an inoculating loop was dipped directly into the preculture and streaked onto a LB agar plate (50 μ g/mL amp, 50 μ g/mL spec, 0.1% arabinose, 10 μ M Na₂SeO₃, 50 μ g/mL kan). For growths observing the effect of Na₂SeO₃ and arabinose on Sec incorporation, the required Na₂SeO₃ and arabinose concentrations were implemented starting at the preculture stage with the same starting colony used for each set of experiments.

GFP fluorescence assay

Plasmids encoding the Sec expression system and sfGFP-M86 variant were transformed into electrocompetent *E. coli* cells (ME6, B-95. $\Delta A\Delta fabR$, or B-95. $\Delta A\Delta fabR\Delta selABC$),^{16,30} plated on LB agar plates (50 $\mu\text{g}/\text{mL}$ amp, 50 $\mu\text{g}/\text{mL}$ spec), and incubated at 37 °C overnight. Single colonies were grown in 0.5 mL LB (50 $\mu\text{g}/\text{mL}$ amp, 50 $\mu\text{g}/\text{mL}$ spec, 1% glucose, 0.1% arabinose, 10 μM Na_2SeO_3) at 37 °C for 8 hours before transferred to a 96-well black plate with clear bottoms. Cultures were mixed 1:1 with fresh media (to a final volume of 150 μL) with and without the addition of 1 mM isopropyl β -D-1-thiogalactopyranoside (IPTG) to induce sfGFP expression. Fluorescence (Ex. 485 nm, Em. 528 nm) and A_{600} readings were taken every 15 minutes for 24 hours at 37 °C on the Synergy HTX Plate Reader (BioTek). Each experiment was performed with a minimum of four biological replicates. The fluorescence readings were divided by the cell densities (A_{600}) at 16 hours and were graphed using GraphPad Prism 9.

In vivo FDH_H activity assay

Plasmids encoding the Sec expression system and *fdhF* were transformed into electrocompetent B-95. $\Delta A\Delta fabR\Delta selABC$ cells, plated on LB agar plates (50 $\mu\text{g}/\text{mL}$ amp, 50 $\mu\text{g}/\text{mL}$ spec), and incubated at 37 °C overnight. Single colonies were grown in 7 mL LB cultures (50 $\mu\text{g}/\text{mL}$ amp, 50 $\mu\text{g}/\text{mL}$ spec, 0.1% arabinose, 10 μM Na_2SeO_3) at 37 °C overnight. A dilution of A_{600} 5.0 and 2-fold serial dilutions were prepared. From each dilution, 5 μL was spotted onto LB agar plates (50 $\mu\text{g}/\text{mL}$ amp, 50 $\mu\text{g}/\text{mL}$ spec, 0.1% arabinose, 10 μM Na_2SeO_3 , 50 mM sodium formate (NaHCOO), 1 μM sodium molybdate (Na_2MoO_4), 10 μM IPTG). Plates were placed inside an anaerobic jar (90% N_2 , 5% H_2 , 5% CO_2) and incubated at 37 °C for 24 hours. A thin layer of LB agar (0.75% agar, 1 mg/mL benzyl viologen di-chloride, 250 mM NaHCOO , 25 mM monopotassium phosphate (KH_2PO_4) [pH 7.0]) was poured over the plates in an anaerobic chamber and imaged after 24 hours.

Expression and purification of *E. coli* Grx1

Expression and purification of C-terminally tagged *E. coli* Grx1 was performed as previously described with minor changes.¹⁵ Briefly, plasmids encoding the Sec expression system and Grx1 variant were transformed into electrocompetent B-95. $\Delta A\Delta fabR\Delta selABC$, plated on LB agar plates (50 $\mu\text{g}/\text{mL}$ amp, 50 $\mu\text{g}/\text{mL}$ spec), and incubated at 37 °C overnight. Grx1 (11Cys/14Ser) and Grx1 (11Ser/14Ser) were co-transformed with the Sec expression plasmid system void of allo-tRNA^{UTu2D}. Single colonies were grown in 10 mL LB (50 $\mu\text{g}/\text{mL}$ amp, 50 $\mu\text{g}/\text{mL}$ spec) at 37 °C overnight and used to inoculate 1 L LB (50 $\mu\text{g}/\text{mL}$ amp, 50 $\mu\text{g}/\text{mL}$ spec, 0.1% arabinose, 10 μM Na_2SeO_3). Cultures were grown at 37 °C until A_{600} 1.2, at which point the temperature was lowered to 20 °C and protein expression was induced with 100 μM IPTG for 20 hours.

All purification steps were performed under anaerobic conditions (90% N_2 , 5% H_2 , 5% CO_2) in an anaerobic tent (Coy Laboratories). Each pellet was resuspended in 18 mL lysis buffer (50 mM sodium phosphate [pH 8.0], 300 mM NaCl, 10% glycerol, 30 mM imidazole) and 2 mL BugBuster® 10X Extraction Reagent (EMD Millipore) along with 2 mM β -mercaptoethanol and 0.05 mg/mL lysozyme. The resuspended cells were incubated at room temperature for 20 minutes, with occasional mixing, and the lysate was centrifuged at 38 000 rpm for 45 minutes at 4 °C. The supernatant was loaded onto 2 mL nickel resin (Ni-NTA Agarose, Qiagen) pre-equilibrated with lysis buffer. The beads were washed with 150 mL lysis buffer and eluted in 1 mL fractions with elution buffer (50 mM sodium phosphate [pH 8.0], 300 mM NaCl, 10% glycerol, 230 mM imidazole). Protein elution was monitored using the Bio-Rad Protein Assay Dye. Elutions were concentrated and buffer exchanged to the storage buffer (50 mM sodium phosphate [pH 8.0], 300 mM NaCl, 10% glycerol) using Amicon® Ultra Centrifugal Filters (Merck Millipore) and stored at –80 °C.

Grx1 glutathione oxidoreductase activity assay

The assay was performed as previously described.¹⁵ Briefly, 35 μL 20 mM β -hydroxyethylene disulfide (HED, final is 0.7 mM) was preincubated with 950 μL buffer (1 mM reduced glutathione, 100 mM Tri-HCl [pH 8.0], 2 mM EDTA, 1 mg/mL bovine serum albumin (BSA), 0.4 mM nicotinamide adenine dinucleotide phosphate reduced (NADPH), 6 $\mu\text{g}/\text{mL}$ glutathione reductase) for 2 minutes at room temperature. The reaction was initiated with the addition of 10, 25, or 50 nM Grx1 variant (in triplicate) and the consumption of NADPH was measured at 340 nm every 30 seconds for 3 minutes. The change in absorbance over time was calculated from 1 to 2 minutes and averaged between the three measurements, followed by buffer subtraction. This was adjusted to a change in nmol of NADPH using the extinction coefficient ($\epsilon = 0.00622 \mu\text{M}^{-1}\text{cm}^{-1}$) and then plotted against the concentration of Grx1 used. The slope and error of this line were used to calculate the activity of the enzyme (in μmol of NADPH/minute/mg protein) using the molecular weight of Grx1 (10 804 Da).

Expression and purification of human GPx1

Expression and purification of human GPx1 was performed as described above for *E. coli* Grx1.

Glutathione peroxidase activity assay with GPx1 variants

GPx1 peroxidase activity was assessed in a 96-well plate using a Glutathione Peroxidase Assay Kit (Cayman Chemical). GPx1 samples diluted in GPX Sample Buffer (50 mM Tris-HCl [pH 7.6], 5 mM ethylenediaminetetraacetic acid (EDTA), 1 mg/mL BSA) were analyzed according to the manufacturer's protocol. Depending on the sample, 0.1–3 µg of protein was used to achieve a decrease in absorbance between 0.02 and 0.135 per minute. Consumption of NADPH was measured at 340 nm every minute for 10 minutes on the Synergy HT Plate Reader (BioTek). A positive control of bovine erythrocyte GPx and a blank for background subtraction were included. Calculations for GPx1 activity were performed as in the manufacturer's protocol and expressed per mg of enzyme used in the reaction. All reactions were performed in triplicate.

Intact mass spectrometry of GPx1 Sec variants

GPx1 and Grx1 Sec variants were sent to Bioinformatics Solutions, Inc (Canada) for intact mass analysis to quantify Sec incorporation. Protein samples were reduced with DTT³⁴ before LC-MS was performed on a Thermo Scientific Orbitrap Fusion Lumos Tribrid mass spectrometer, equipped with a heated electrospray ionization source (H-ESI) in positive ion mode with a Thermo Fisher Ultimate 3000 RSLC nano HPLC System. On H-ESI source, sheath gas was set to 2 arbitrary units (arb), and auxiliary gas was set to 6.7 arb. The vaporizer temp was at 200 °C. The sample was analyzed on a MAbPac RP, 4 µM, 3.0X50 mm analytical column (ThermoFisher, San Jose, CA), held at 70 °C. Protein was eluted at a rate of 500 µL/min for a 10 min gradient. 0–7 mins: 10–70% acetonitrile + 0.1% formic acid; 7–8.2 mins: 95% acetonitrile + 0.1% formic acid, 8.2–10 mins: 20% acetonitrile + 0.1% formic acid. MS spectra were acquired using full scans at 7500 resolution in the orbitrap within a range of 700–2200 *m/z*. The maximum injection time was limited to 50 ms, with an AGC target of 4e6. Ten micro scans were employed, and the RF lens was set to 50%. 15 V of insource CID was applied.

Thermo BioPharma Finder™ 4.1 (ThermoFisher Scientific) was used for intact mass deconvolution and peak identification.

CRedit authorship contribution statement

Christina Z. Chung: Conceptualization, Methodology, Investigation, Visualization. **Natalie Krahn:** Conceptualization, Methodology, Investigation, Visualization. **Ana Crnković:** Conceptualization, Methodology, Investigation.

Dieter Söll: Conceptualization, Supervision, Funding acquisition.

Acknowledgements

We thank Henning D. Mootz (Münster, Germany) for inspired advice and the gift of M86 DnaB constructs. We are grateful to Jonathan Fischer, Jeffery Sharp, Oscar Vargas-Rodriguez, and Kyle Hoffman (Bioinformatics Solutions, Inc) for experimental advice and mass spectrometry support.

Funding

This work was supported by grants from the National Institute of General Medical Sciences (R35GM122560 to D.S.), and, for the genetic studies, the Department of Energy Office of Basic Energy Sciences (DE-FG0298ER2031 to D.S.). Christina Z. Chung holds a Postdoctoral Fellowship from the Natural Sciences and Engineering Research Council of Canada (NSERC).

Declaration of Competing Interest

The authors declare that they have no conflict of interest.

Appendix A. Supplementary material

Supplementary data to this article can be found online at <https://doi.org/10.1016/j.jmb.2021.167199>.

Received 25 June 2021;

Accepted 4 August 2021;

Available online 16 August 2021

Keywords:

genetic code expansion;
tRNA;
selection method;
screening method;
protein splicing

† Current address: Laboratory for Molecular Biology and Nanobiotechnology, National Institute of Chemistry, Hajdrihova 19, Ljubljana, Slovenia.

@NatalieKrahn_13  (N. Krahn)

References

- Schmidt, R.L., Simonović, M., (2012). Synthesis and decoding of selenocysteine and human health. *Croat. Med. J.*, **53**, 535–550.
- Kang, D., Lee, J., Wu, C., Guo, X., Lee, B.J., Chun, J.S., Kim, J.H., (2020). The role of selenium metabolism and

- selenoproteins in cartilage homeostasis and arthropathies. *Exp. Mol. Med.*, **52**, 1198–1208.
3. Reich, H.J., Hondal, R.J., (2016). Why nature chose selenium. *ACS Chem. Biol.*, **11**, 821–841.
 4. Maroney, M.J., Hondal, R.J., (2018). Selenium versus sulfur: Reversibility of chemical reactions and resistance to permanent oxidation in proteins and nucleic acids. *Free Radic. Biol. Med.*, **127**, 228–237.
 5. Snider, G.W., Ruggles, E., Khan, N., Hondal, R.J., (2013). Selenocysteine confers resistance to inactivation by oxidation in thioredoxin reductase: comparison of selenium and sulfur enzymes. *Biochemistry*, **52**, 5472–5481.
 6. Arai, K., Takei, T., Okumura, M., Watanabe, S., Amagai, Y., Asahina, Y., Moroder, L., Hojo, H., et al., (2017). Preparation of selenoinsulin as a long-lasting insulin analogue. *Angew. Chem. Int. Ed. Engl.*, **56**, 5522–5526.
 7. Metanis, N., Hilvert, D., (2014). Natural and synthetic selenoproteins. *Curr. Opin. Chem. Biol.*, **22**, 27–34.
 8. Evans, R.M., Krahn, N., Murphy, B.J., Lee, H., Armstrong, F.A., Söll, D., (2021). Selective cysteine-to-selenocysteine changes in a [NiFe]-hydrogenase confirm a special position for catalysis and oxygen tolerance. *Proc. Natl. Acad. Sci. U S A*, **118**
 9. Giesler, R.J., Erickson, P.W., Kay, M.S., (2020). Enhancing native chemical ligation for challenging chemical protein syntheses. *Curr. Opin. Chem. Biol.*, **58**, 37–44.
 10. Liu, J., Chen, Q., Rozovsky, S., (2018). Selenocysteine-mediated expressed protein ligation of SELENOM. *Methods Mol. Biol.*, **1661**, 265–283.
 11. Pegoraro, S., Fiori, S., Rudolph-Bohner, S., Watanabe, T. X., Moroder, L., (1998). Isomorphous replacement of cystine with selenocystine in endothelin: oxidative refolding, biological and conformational properties of [Sec3, Sec11, Nle7]-endothelin-1. *J. Mol. Biol.*, **284**, 779–792.
 12. Metanis, N., Hilvert, D., (2015). Harnessing selenocysteine reactivity for oxidative protein folding. *Chem. Sci.*, **6**, 322–325.
 13. Labunskyy, V.M., Hatfield, D.L., Gladyshev, V.N., (2014). Selenoproteins: molecular pathways and physiological roles. *Physiol. Rev.*, **94**, 739–777.
 14. Cheng, Q., Arner, E.S., (2017). Selenocysteine insertion at a predefined UAG codon in a release factor 1 (RF1)-depleted *Escherichia coli* host strain bypasses species barriers in recombinant selenoprotein translation. *J. Biol. Chem.*, **292**, 5476–5487.
 15. Aldag, C., Bröcker, M.J., Hohn, M.J., Prat, L., Hammond, G., Plummer, A., Söll, D., (2013). Rewiring translation for elongation factor Tu-dependent selenocysteine incorporation. *Angew. Chem. Int. Ed. Engl.*, **52**, 1441–1445.
 16. Mukai, T., Sevostyanova, A., Suzuki, T., Fu, X., Söll, D., (2018). A facile method for producing selenocysteine-containing proteins. *Angew. Chem. Int. Ed. Engl.*, **57**, 7215–7219.
 17. Miller, C., Bröcker, M.J., Prat, L., Ip, K., Chirathivat, N., Feiock, A., Veszprémi, M., Söll, D., (2015). A synthetic tRNA for EF-Tu mediated selenocysteine incorporation *in vivo* and *in vitro*. *FEBS Lett.*, **589**, 2194–2199.
 18. Thyer, R., Robotham, S.A., Brodbelt, J.S., Ellington, A.D., (2015). Evolving tRNA(Sec) for efficient canonical incorporation of selenocysteine. *J. Am. Chem. Soc.*, **137**, 46–49.
 19. Tharp, J.M., Ad, O., Amikura, K., Ward, F.R., Garcia, E.M., Cate, J.H.D., Schepartz, A., Söll, D., (2020). Initiation of protein synthesis with non-canonical amino acids *in vivo*. *Angew. Chem. Int. Ed. Engl.*, **59**, 3122–3126.
 20. Kwok, H.S., Vargas-Rodriguez, O., Melnikov, S.V., Söll, D., (2019). Engineered aminoacyl-tRNA synthetases with improved selectivity toward noncanonical amino acids. *ACS Chem. Biol.*, **14**, 603–612.
 21. Mandrand-Berthelot, M.-A., Wee, M.Y.K., Haddock, B.A., (1978). An improved method for the identification and characterization of mutants of *Escherichia coli* deficient in formate dehydrogenase activity. *FEMS Microbiol. Lett.*, **4**, 37–40.
 22. Thyer, R., Shroff, R., Klein, D.R., d'Oelsnitz, S., Cotham, V. C., Byrom, M., Brodbelt, J.S., Ellington, A.D., (2018). Custom selenoprotein production enabled by laboratory evolution of recoded bacterial strains. *Nature Biotechnol.*, **36**, 624–631.
 23. Rodriguez, E.A., Tran, G.N., Gross, L.A., Crisp, J.L., Shu, X., Lin, J.Y., Tsien, R.Y., (2016). A far-red fluorescent protein evolved from a cyanobacterial phycobiliprotein. *Nature Methods*, **13**, 763–769.
 24. Haruna, K., Alkazemi, M.H., Liu, Y., Söll, D., Englert, M., (2014). Engineering the elongation factor Tu for efficient selenoprotein synthesis. *Nucleic Acids Res.*, **42**, 9976–9983.
 25. Appleby-Tagoe, J.H., Thiel, I.V., Wang, Y., Wang, Y., Mootz, H.D., Liu, X.Q., (2011). Highly efficient and more general *cis*- and *trans*-splicing inteins through sequential directed evolution. *J. Biol. Chem.*, **286**, 34440–34447.
 26. Di Ventura, B., Mootz, H.D., (2019). Switchable inteins for conditional protein splicing. *Biol. Chem.*, **400**, 467–475.
 27. Friedel, K., Popp, M.A., Matern, J.C.J., Gazdag, E.M., Thiel, I.V., Volkmann, G., Blankenfeldt, W., Mootz, H.D., (2019). A functional interplay between intein and extein sequences in protein splicing compensates for the essential block B histidine. *Chem. Sci.*, **10**, 239–251.
 28. Amitai, G., Callahan, B.P., Stanger, M.J., Belfort, G., Belfort, M., (2009). Modulation of intein activity by its neighboring extein substrates. *Proc. Natl. Acad. Sci. U. S. A.*, **106**, 11005–11010.
 29. Wu, H., Xu, M.Q., Liu, X.Q., (1998). Protein trans-splicing and functional mini-inteins of a cyanobacterial DnaB intein. *BBA*, **1387**, 422–432.
 30. Mukai, T., Hoshi, H., Ohtake, K., Takahashi, M., Yamaguchi, A., Hayashi, A., Yokoyama, S., Sakamoto, K., (2015). Highly reproductive *Escherichia coli* cells with no specific assignment to the UAG codon. *Sci. Rep.*, **5**, 9699.
 31. Rocher, C., Lalanne, J.L., Chaudiere, J., (1992). Purification and properties of a recombinant sulfur analog of murine selenium-glutathione peroxidase. *Eur. J. Biochem.*, **205**, 955–960.
 32. Liu, J., Zheng, F., Cheng, R., Li, S., Rozovsky, S., Wang, Q., Wang, L., (2018). Site-specific incorporation of selenocysteine using an expanded genetic code and palladium-mediated chemical deprotection. *J. Am. Chem. Soc.*, **140**, 8807–8816.
 33. Rosano, G.L., Ceccarelli, E.A., (2014). Recombinant protein expression in *Escherichia coli*: advances and challenges. *Front. Microbiol.*, **5**, 172.
 34. Hansen, R.E., Winther, J.R., (2009). An introduction to methods for analyzing thiols and disulfides: Reactions,

- reagents, and practical considerations. *Anal. Biochem.*, **394**, 147–158.
35. Stogios, P.J., Spanogiannopoulos, P., Evdokimova, E., Egorova, O., Shakya, T., Todorovic, N., Capretta, A., Wright, G.D., et al., (2013). Structure-guided optimization of protein kinase inhibitors reverses aminoglycoside antibiotic resistance. *Biochem. J.*, **454**, 191–200.
36. Pédelacq, J.D., Cabantous, S., Tran, T., Terwilliger, T.C., Waldo, G.S., (2006). Engineering and characterization of a superfolder green fluorescent protein. *Nature Biotechnol.*, **24**, 79–88.